

Influence of CoO and Al₂O₃ on the Phase Partitioning of ZrO₂–3 mol% Y₂O₃

Y. H. Chiou & S. T. Lin

Mechanical Engineering Department, National Taiwan Institute of Technology, Taipei, Taiwan

(Received 23 February 1995; accepted 16 June 1995)

Abstract: Tetragonal zirconia polycrystal doped with 1.5 wt% CoO and 1.5 wt% Al₂O₃ showed large and faceted CoAl₂O₄ spinel grains existing in clusters and large monoclinic zirconia grains. Major stages of microstructural evolution during sintering included (1) formation of spinel as a result of preferred segregation of CoO to Al₂O₃ phase, (2) exudation of liquid phase to grain junctions among faceted spinel grains and zirconia grains, and (3) growth of spinel grains and the zirconia grains adjacent to the spinel phase.

1 INTRODUCTION

Tetragonal zirconia polycrystal (TZP) is gaining popularity as an engineering ceramic because of its excellent mechanical properties, especially a high fracture toughness value. The high fracture toughness is associated with the retention of a tetragonal phase, which transforms into monoclinic phase under applied stress by various mechanisms.¹ Stabilizers such as MgO, CaO, Y₂O₃ and CeO₂ are used to retain the tetragonal phase after sintering, among which yttria is the most commonly used.

The retention of tetragonal phase after sintering is possible if the grain size of the dense polycrystalline materials is smaller than a critical size, which depends on the yttria content.¹ However, the omnipresence of liquid phase arising from powder impurities or additives caused the repartition of yttria during sintering, whose effect on growth of zirconia grains had been controversial. For example, composition difference of yttria from grain to grain as a result of the presence of a liquid phase caused reduced grain growth.² Similarly, segregation of an impurity layer or yttria to the grain boundaries results in reduced grain boundary mobility through an impurity drag mechanism,³ or space charge drag mechanism.⁴ On the other hand, repartition of yttria to the boundaries of zirconia grains, which was faster in an impurity richer powder, caused enhanced grain growth when the phase repartition

had finished.⁵ In addition to grain growth behaviour, impurities or additives forming liquid phase also affect the high temperature properties. For example, a significant difference in the superplastic behaviour for TZPs having different impurity levels was attributed to the difference in the chemical composition, viscosity, and repartition of constituents of the grain boundary liquid phase.⁶

Much of the interest in duplex structures has focused on the control of grain growth, which not only improves the mechanical properties,⁷ but also improves the superplasticity by resisting grain coarsening at elevated temperatures.⁴ However, the presence of a small content of liquid phase in alumina–TZP duplex composites enhanced the grain growth of both phases by forming liquid channels between grain boundaries, in which both alumina and zirconia are soluble.⁸ On the other hand, the existence of a liquid phase in the sintering of Al₂O₃–SiC composites enables the formation of a homogeneous microstructure due to the elimination of stresses during thermal treatment.⁹

Doping of transitional metal oxides has been applied to change the properties of oxide ceramics. Examples include modifying pore structure,¹⁰ altering colour,¹¹ and improving high temperature superplastic behaviour.^{4,12} The success of these examples depends strongly on the control of microstructural evolution at elevated temperatures. The incentive of this study was to alter the colour

of TZP by doping a small content of alumina and cobalt oxide. The microstructural evolution of a duplex structure with the presence of a liquid phase during sintering was examined and correlated with the sintered properties.

2 EXPERIMENTAL

Both doped and undoped zirconia powders were studied in a parallel manner. A commercial grade TZP powder (ZrO_2 -3 mol% Y_2O_3 , HSY-3.0, Daiichi Kigenso Kagaku Kogyo Co. Ltd., Japan) was used as the starting powder. The purity of this powder was 99.4%. It had an average particle size of $0.6 \mu\text{m}$ and a specific surface area of $6.9 \text{ m}^2/\text{g}$. The composition of the doped TZP was ZrO_2 -3 mol% Y_2O_3 , doped with 1.5 wt% (2.4 mol%) CoO and 1.5 wt% (1.8 mol%) Al_2O_3 . The CoO powder was precipitated from CoCl_2 water solution with diluted ammonia ($\text{pH} = 8.0$), followed by washing the precipitate with deionized water. The precipitate was then calcined at 200°C and ground. The mean particle size was $3 \mu\text{m}$. The alumina powder was a commercial grade powder (99.8% pure, AES-11, Sumitomo Chemical, Japan), which had a mean particle size of $0.5 \mu\text{m}$ and grain size of $0.3 \mu\text{m}$.

The doped TZP powder was prepared by wet ball-milling the powders in a plastic jar for 8 h, using alumina balls (99.7% pure). Specimens having the approximate dimensions of 16 mm diameter and 5 mm height were uniaxially compacted at a pressure of 30 MPa. The specimens were then sintered in air. The sintering profile was a ramp of 3 K/min to 500°C , held for 30 min, followed by a ramp of 10 K/min to the sintering temperatures (1300 – 1600°C), held for 1 h.

X-ray diffraction (XRD) patterns of the as-sintered specimens were recorded using nickel filtered $\text{CuK}\alpha$ radiation. The relative abundance of monoclinic phase (M) was determined using the following relationship:¹³

$$M = \frac{I_m(111)}{I_m(111) + I_t(111) + \frac{1}{8}I_c(111)} \quad (1)$$

where $I_m(111)$ denotes the intensity of the monoclinic (111) peak, $I_t(111)$ refers to the intensity of the tetragonal (111) peak, and $I_c(111)$ represents the intensity of the cubic (111) peak. In all patterns, $I_c(111)$ was zero because of no detectable cubic (400) peak.

The density of the sintered specimens was measured by Archimedes principle. The specimens were then cold mounted and relief polished. The hard-

ness and the fracture toughness of the sintered specimens were measured using Vickers diamond micro-indenter with loads of 9.8 N and 245 N, respectively. The hardness and toughness were the average of five tests. The fracture toughness (K_{Ic}) was calculated from the following formula:¹⁴

$$K_{Ic}\Phi = 0.48\left(\frac{c}{a}\right)^{-1.5}Ha^{0.5} \quad (2)$$

where Φ is a constraint factor and is approximately equal to 3, c is one half crack length, a is one half indent diagonal, and H is microhardness based on Vickers test. The polished surface was thermally etched at 1300°C for 2 h in air. The microstructure observation was conducted using scanning electron microscope (SEM). The grain size reported was the average of more than 500 grains, using an image analysis system (Q520, Cambridge). Additionally, microstructure and composition of the intergranular glass phase was analysed using transmission electron microscope (TEM) equipped with an energy dispersive X-ray analyser (EDXA).

3 RESULTS AND DISCUSSION

3.1 Formation of CoAl_2O_4 spinel

Figure 1 compares the XRD patterns of undoped TZP and doped TZP sintered at 1300°C . The

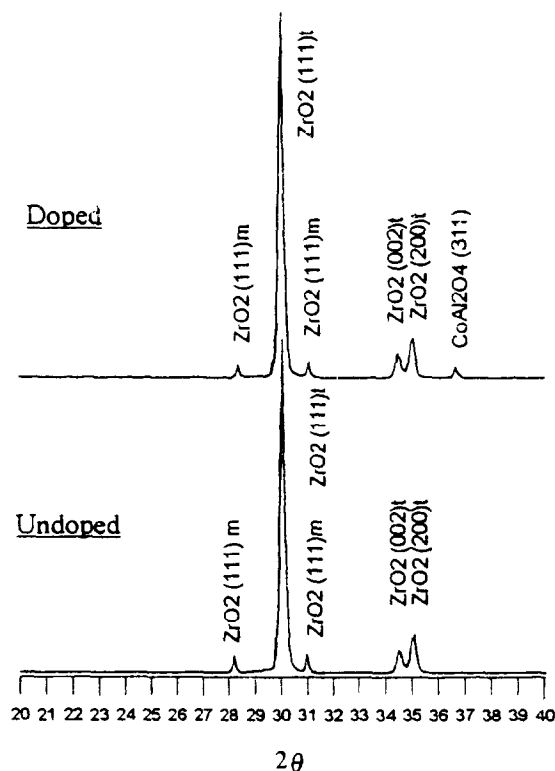


Fig. 1. XRD patterns of doped and undoped TZPs sintered at 1300°C .

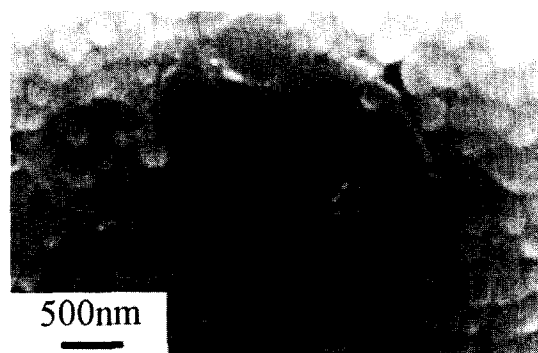


Fig. 2. SEM micrograph of spinel phase located in zirconia matrix for doped TZP sintered at 1300°C.

difference between these two patterns was the existence of a CoAl_2O_4 (311) peak at 36.1° in the doped TZP. The other diffraction peaks of CoAl_2O_4 were weaker than (311), and either overlapped with monoclinic zirconia (111) peak at 31.1° or disappeared as background signals. The

CoAl_2O_4 spinel had formed while individual CoO and Al_2O_3 could not be identified at 1300°C. Figure 2 shows the microstructure of doped TZP sintered at 1300°C, in which the spinel grains had a mean grain size similar to that of the starting alumina grains ($0.3 \mu\text{m}$), whereas no spinel grain having a size similar to that of the starting CoO grains ($2 \mu\text{m}$) was observed. This observation indicated that mass transfer of CoO toward Al_2O_3 was responsible for the formation of CoAl_2O_4 spinel. Since the starting powders were ball-milled, the distribution of CoO and Al_2O_3 should have been very uniform in the zirconia matrix and could not have all coupled together. Therefore, mass transfer of CoO took place either by vaporization and condensation or diffusion of CoO through the grain boundaries between zirconia grains to the Al_2O_3 grains. Mass transfer of CoO through the vapour phase was possible due to its high vapour pressure at elevated temperatures (e.g. 9×10^{-18} atm at

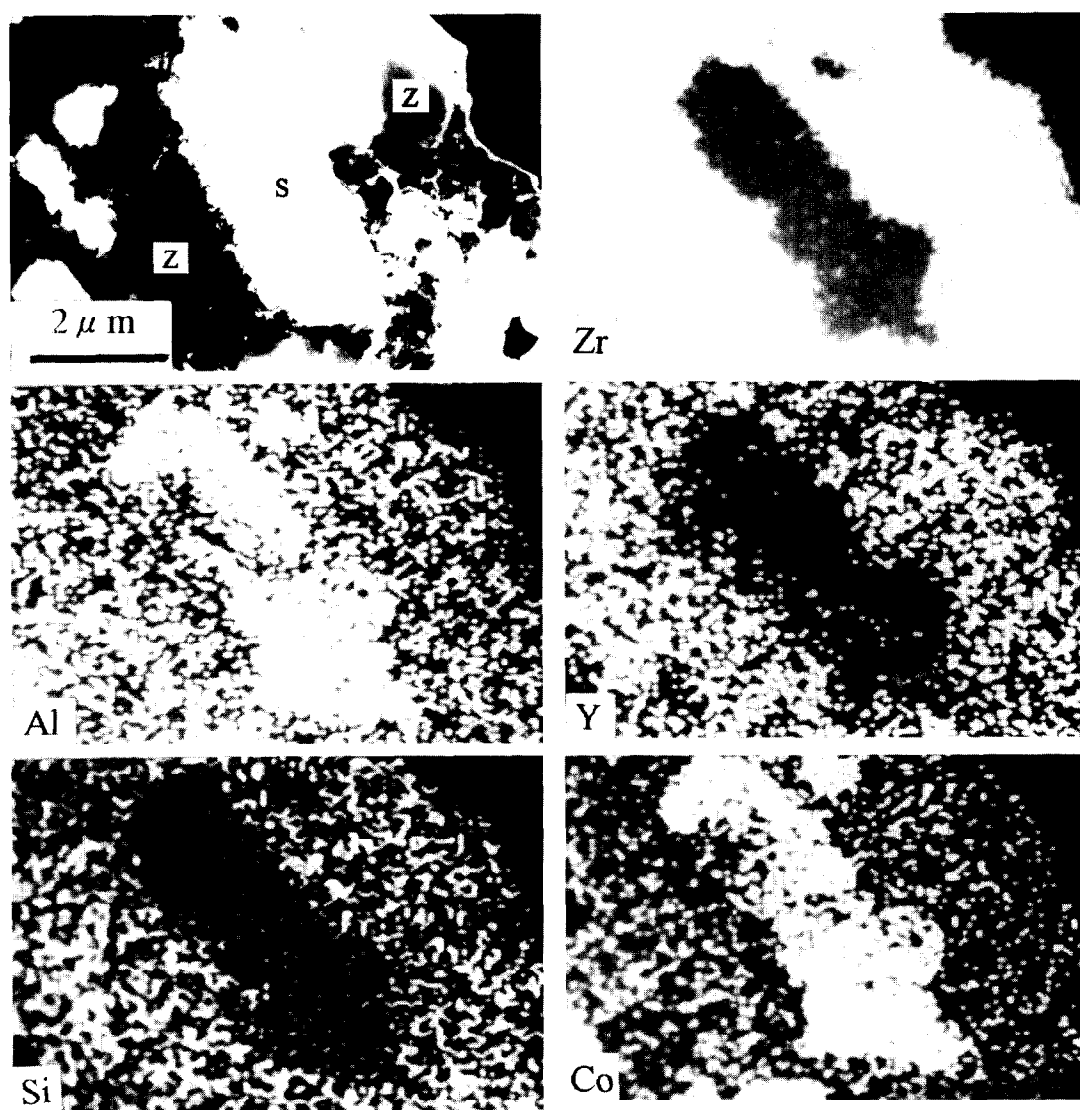


Fig. 3. TEM bright field micrograph and corresponding EDXA dot maps of constituents for doped TZP sintered at 1350°C. (S = spinel, Z = zirconia)

727°C),¹⁵ and could be observed in the alumina substrate whose colour was altered into a blue colour. However, it was not the sole mechanism responsible for the mass transfer of CoO to Al_2O_3 because condensation of CoO vapour on both Al_2O_3 and ZrO_2 particle surfaces was possible. Preferred segregation of CoO to Al_2O_3 also required the mass transfer of CoO to Al_2O_3 by revaporization–condensation and by diffusion through the intergranular liquid channels in the zirconia matrix.

The spare CoO was lost by vaporization during sintering because the initial mole ratio of CoO to Al_2O_3 was 2.4 mol% to 1.8 mol%. Differential thermal analysis and thermal gravimetric analysis of the doped TZP indicated an endothermic peak and a weight loss peak at 930°C. Therefore, mass transfer of CoO through vapour phase should have been very active in the temperature range studied. Additionally, the formation of spinel was energetically favourable because the enthalpies of formation of CoAl_2O_4 from CoO and Al_2O_3 at 1000°C and 1350°C are -29 kJ/mol and -26 kJ/mol, respectively.¹⁶ Figure 3 shows the EDXA dot maps for Al, Co, Y, Zr and Si. CoO did not totally dissolve into the liquid phase as was expected for a TZP only doped with CoO,⁴ but it preferentially segregated to Al_2O_3 and formed CoAl_2O_4 spinel. It has been a long practice to use some oxides to stabilize the cobalt blue colour by forming new compounds, to avoid formation of bubbles in

glazes as a result of vaporization of CoO.¹⁷ Similarly, the existence of alumina assisted the stabilization of CoO in TZP by forming a spinel phase.

3.2 Formation of liquid phase

The existence of silica as an impurity of powders results in formation of liquid phase in different ceramic systems.^{4,18–22} Zirconia usually contains a certain amount of Si impurity, which is localized in the intergranular grain boundary liquid phase after sintering.^{4,22} An eutectic temperature for the ternary Al_2O_3 – SiO_2 –CoO exists at 1339°C,²³ while that for the ternary ZrO_2 – SiO_2 – Y_2O_3 exists at 1350°C.⁴ Dissolution of the other components into these ternary liquid phases should have further reduced the eutectic temperature or liquid phase formation temperature. Figure 4 shows TEM micrographs of a doped TZP specimen sintered at 1350°C. Liquid phase located near the grain boundaries and grain junctions can be observed. EDXA composition analysis shown in Fig. 5 indicated that the liquid phase located in grain junctions was composed of various concentrations of SiO_2 , Y_2O_3 , Al_2O_3 and ZrO_2 , depending on the location of the liquid phase. These four components are commonly observed as the constituents of the grain boundary liquid phase of undoped TZP.⁵ The CoO concentration in the liquid phase was so low that its signal could not be differentiated from the background signal even for the liquid phase located at the grain junctions among spinel grains, but its distribution in the liquid phase could be observed in the EDXA dot maps (Fig. 3). As indicated previously, CoO forms an eutectic

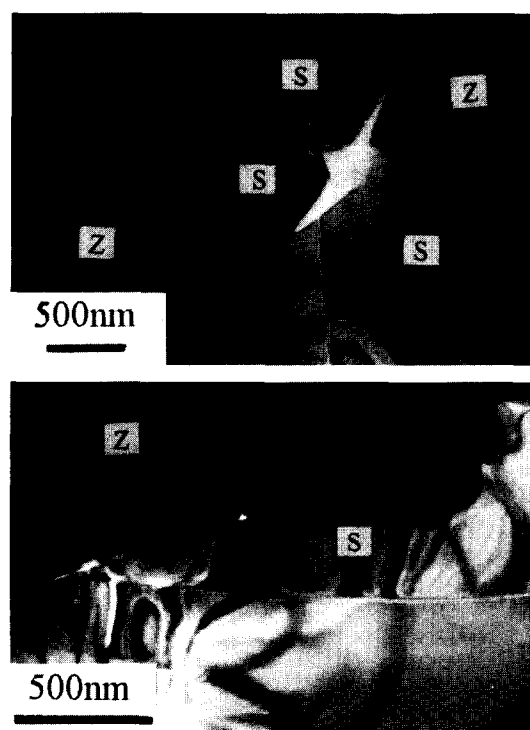


Fig. 4. TEM bright field micrographs of doped TZP sintered at 1350°C. (S = spinel, Z = zirconia)

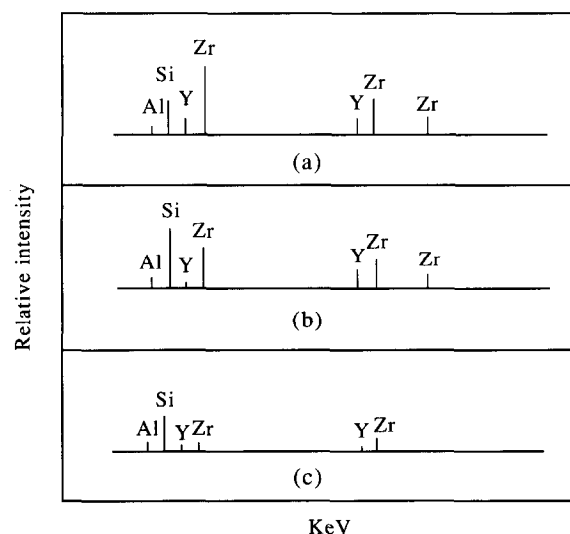


Fig. 5. EDXA analysis of grain junction liquid pockets surrounded by different phases of grains for doped TZP sintered at 1350°C: (a) among TZP grains; (b) among TZP and spinel grains; (c) among spinel grains.

liquid phase at 1339°C with SiO_2 and Al_2O_3 , but its concentration in the liquid phase was very low. Therefore, the lack of CoO in the liquid phase indicated that CoO had a stronger affinity of reacting with Al_2O_3 or vaporization than participating in forming the liquid phase.

Phase repartition of Y_2O_3 in TZP was significant at elevated sintering temperatures or for an extended anneal period, in which Y_2O_3 preferentially segregated to the grain boundary liquid phase.⁵ Such a phase repartition phenomenon is promoted by a high impurity content (especially by alumina), an elevated sintering temperature, or an extended annealing time.⁵ In the EDXA analysis shown in Fig. 5, the yttria signal was strong for the liquid phase located in zirconia grain junctions, while insignificant for the liquid phase located in spinel grain junctions. This observation indicated that the partition of yttria occurred only locally near the zirconia grains at this temperature (1350°C). In fact, it takes a much longer time at higher temperatures to reach the plateau of yttria partition.^{5,24}

It was also observed systematically in TEM micrographs of doped TZP sintered at 1350°C that the frequency of observing grain junction liquid phase located among spinel grains and zirconia grains was much higher than that among zirconia grains and zirconia grains. This inhomogeneity was a result of the growth and gradual faceting of spinel grains, which exuded liquid phase from spinel-spinel grain boundaries to spinel-zirconia grain junctions (Fig. 4). Such a phenomenon was similar to that commonly observed in liquid phase sintering²⁵ or that occurred in TZP where exudation of liquid phase from faceted zirconia grains in TZP to grain junctions of rounded grains prevailed for a long thermal anneal.^{5,26} Although the liquid phase was abundant near the spinel grains,

the sintered density of the doped TZP was only slightly improved with respect to the undoped TZP at temperatures lower than 1350°C , as shown in Fig. 6. At higher temperatures the residual porosity was difficult to remove during sintering, as a result of intensive vaporization of CoO phase. Accordingly, the sintered density of the doped TZP decreased with increased sintering temperature.

3.3 Growth of spinel and zirconia grains

The growth of spinel grains took place in a manner similar to that commonly observed in liquid phase sintering,²⁵ i.e. either by dissolution and precipitation, or by coalescence. Figure 7 shows an SEM micrograph for a specimen sintered at 1400°C , in which growth of spinel grains by coalescence was obvious. The growth of the spinel grains was accompanied by grain shape faceting, which resulted in the shape accommodation of the spinel grain and the exudation of liquid phase out of the spinel-spinel grain boundaries (Fig. 4).

Following the growth of the spinel grains isolated in the zirconia matrix, the growth of the spinel phase continued at higher sintering temperatures. The dimensions of the spinel clusters increased while the population decreased with higher sintering temperatures, as shown in Fig. 8. This was a typical consequence of Ostwald ripening. Since the solubility of aluminium ion and cobalt ion in the zirconia matrix are very low,²³ the further growth of the spinel grains occurred by a long-range mass transfer through the liquid channels located between zirconia grains, similar to that observed in sintering an alumina-zirconia duplex composite.⁸

The distribution and component concentration of liquid phase was macroscopically inhomogeneous at 1350°C . The liquid phase was abundant near the spinel grains where it was also rich with

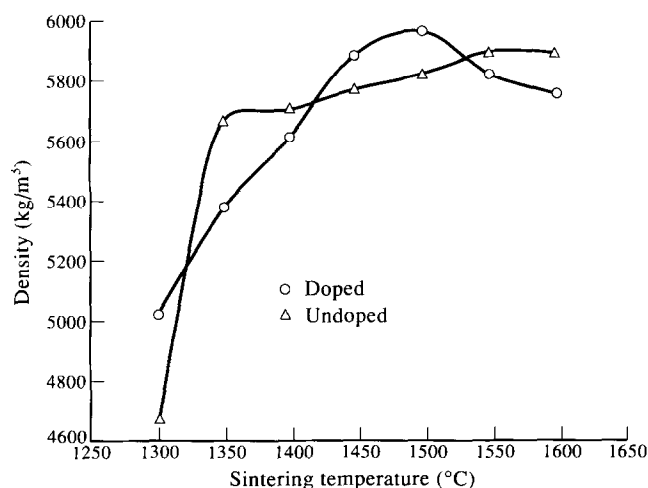


Fig. 6. Variation of sintered density with sintering temperature for doped and undoped TZPs.



Fig. 7. SEM micrograph of doped TZP sintered at 1400°C , showing grain faceting of spinel phase and grain growth of spinel by coalescence.

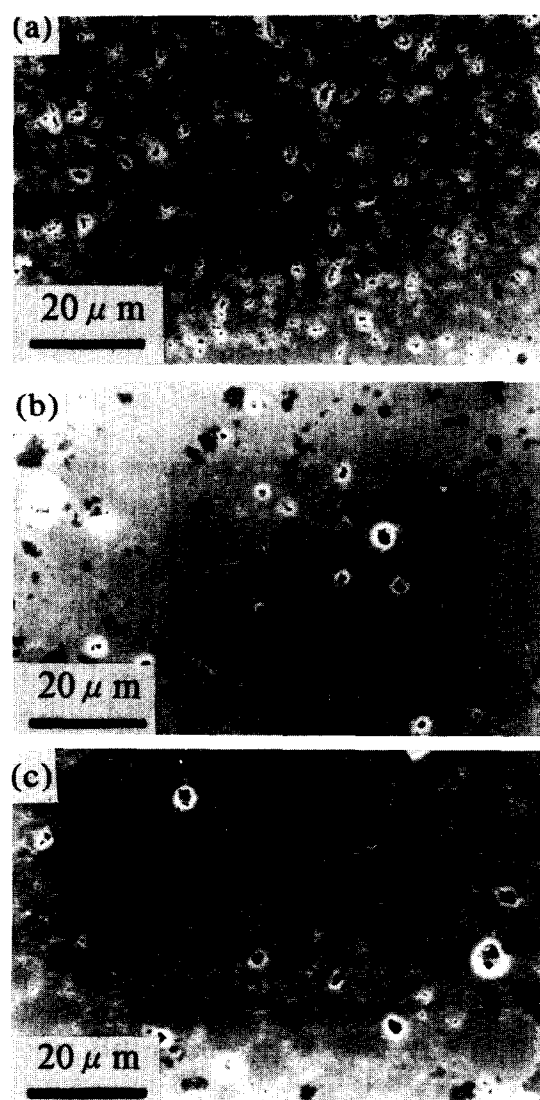


Fig. 8. Growth in size but decrease in population of spinel clusters in zirconia matrix with increase of sintering temperature. (a) 1300°C, (b) 1450°C, (c) 1600°C.

aluminium ions. The dissolution of aluminium ions in the liquid phase is responsible for the enhancement of the amount and reactivity (i.e. solution and precipitation) of the liquid phase.²² The liquid phase therefore promoted the growth of the zirconia grains adjacent to the faceted spinel grains, which can be observed in the micrographs for specimens sintered at 1500°C, shown in Fig. 9. Figure 10 shows the average size and the largest size of zirconia grains for doped and undoped TZPs sintered at different temperatures. The zirconia grains away from the spinel phase for the doped specimens were very similar in size to those of the undoped specimens, whereas the zirconia grains adjacent to the spinel phase grew at lower temperatures and were much larger in size. The effect of impurities on the grain growth of zirconia in Y-TZP was concluded differently in literature. For example, it was found that grain growth rate

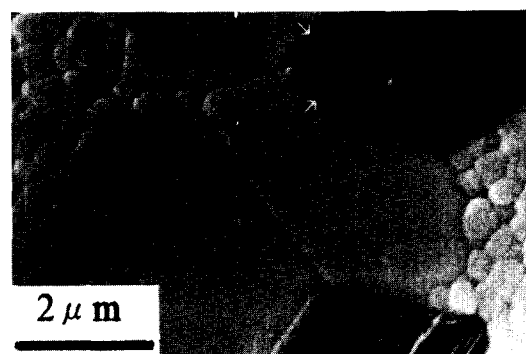


Fig. 9. SEM micrograph of doped TZP sintered at 1500°C, showing the growth of zirconia grains adjacent to the spinel phase.

of zirconia was not affected by the impurity during the yttria repartition stage, while it was enhanced by the presence of a liquid phase when the phase repartition stage finished.⁵ On the other hand, several divalent and trivalent cations were shown to segregate to the grain boundary of TZP, which in turn reduced the grain boundary energy and mobility and, therefore, grain growth rate.⁴ As a result, the grain boundary strength at elevated temperatures was not impaired and the superplastic deformation behaviour of TZP was improved. In this study, with the addition of Al_2O_3 , CoO did not segregate to the grain boundaries but instead formed a spinel phase with alumina and exuded the liquid phase to the boundaries of zirconia grains.

Concurrent with the growth of the zirconia grains adjacent to the spinel phase and the repartition of yttria, the large zirconia grains transformed from tetragonal into monoclinic phase. The relative content of monoclinic phase increased, as shown in Fig. 11. A low concentration of monoclinic phase typically existed in the Y-TZP powder,

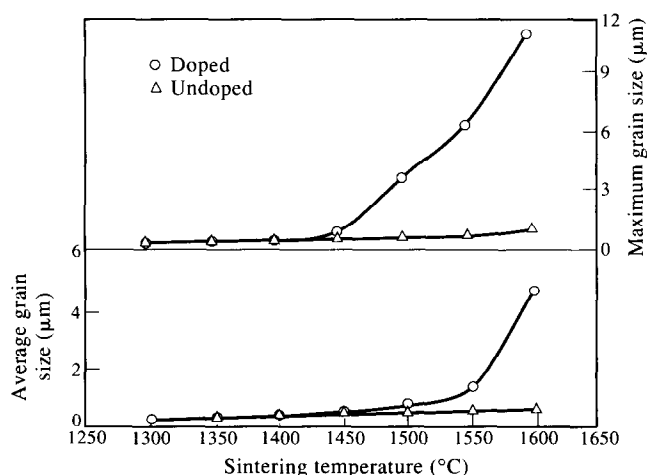


Fig. 10. A comparison of the average grain size and the maximum grain size of zirconia at different sintering temperatures for doped and undoped TZPs.

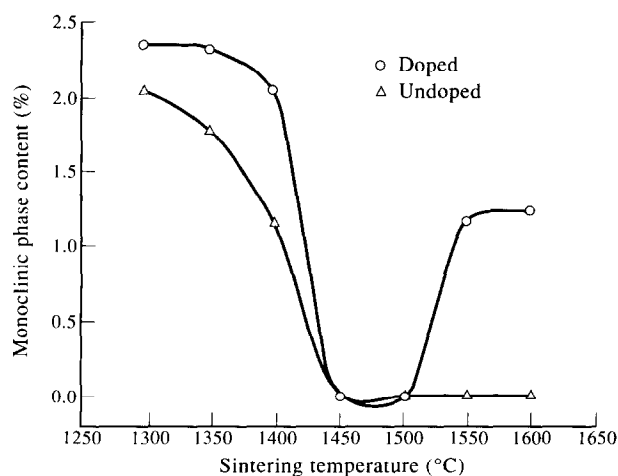


Fig. 11. Variation of relative abundance of monoclinic phase with sintering temperature for doped and undoped TZPs.

whose concentration depends on the powder calcination temperature,²⁷ because the powder calcination temperature was usually low and phase partition of yttria was sluggish.² With the increase of sintering temperature, the monoclinic phase content of the undoped TZP decreased as yttria dissolved into the zirconia grains,²⁴ and remained at very low concentrations at higher temperatures even though slight grain growth of zirconia and phase repartition of yttria had occurred. On the other hand, with the increase of sintering temperature, the monoclinic phase content of doped TZP initially decreased but then increased. The decrease of monoclinic phase was a result of yttria dissolving into the zirconia grains, as indicated previously for undoped zirconia, while the increase of the monoclinic phase at higher temperatures was due to the growth of the zirconia grains adjacent to the spinel phase.

Figure 12 shows the relationship between fracture toughness and sintering temperature for doped and undoped TZP. The fracture toughness for the undoped TZP reached a maximum value at 1450°C, while that for the doped TZP continuously

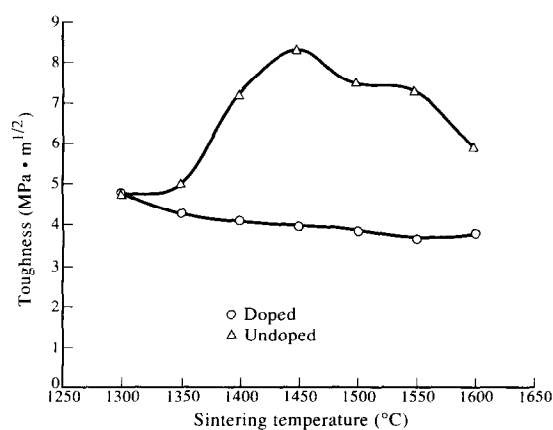


Fig. 12. Variation of fracture toughness with sintering temperature for doped and undoped TZPs.

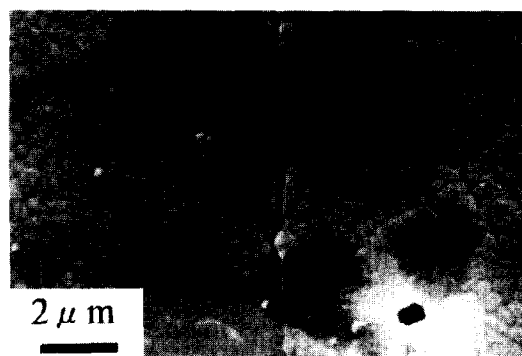


Fig. 13. SEM micrograph for doped TZP sintered at 1550°C, showing induced crack growth through large monoclinic zirconia grains and large faceted spinel phase.

decreased. Such behaviours can be traced to those factors determining the fracture toughness, as indicated in eqn (2). The hardness of TZP was not much affected by the dopants, while the indent diagonal for the doped TZP was slightly smaller than that of undoped TZP. They were not the major factors causing the great difference in fracture toughness. On the other hand, the crack length of the undoped TZP decreased and then increased, whereas that of the doped TZP continuously increased with the increase of sintering temperature. Additionally, the crack length of doped TZP was much longer than that of undoped TZP. Therefore, difference of the crack length in indentation test was the principal factor determining the fracture toughness behaviour shown in Fig. 12. The longer crack length for the doped TZP was a result of transgranular fracture of large monoclinic zirconia grains and induction of crack toward the weak and faceted spinel grains, as shown in Fig. 13. The phase transformation toughening behaviour of TZP disappeared even though the relative abundance of monoclinic phase could be reduced to close to zero (1400–1450°C). Such a significant effect was not observed in a TZP system containing only 0.3 mol% CoO, in which the fracture toughness was not much impaired.⁴

4 CONCLUSION

The effect of doping 1.5 wt% CoO and 1.5 wt% Al_2O_3 on the microstructural evolution and sintered properties of ZrO_2 -3 mol% Y_2O_3 was studied. Results indicated that CoO preferentially segregated to and reacted with Al_2O_3 , forming CoAl_2O_4 spinel at temperatures as low as 1300°C. Additionally, an intergranular liquid phase primarily consisting of SiO_2 , Al_2O_3 , Y_2O_3 and ZrO_2 was formed. This liquid phase promoted the grain growth and grain faceting of CoAl_2O_4 spinel,

which in turn exuded the liquid phase to the grain boundaries between spinel grains and zirconia grains after shape accommodation of the faceted spinel grains. The exuded liquid phase promoted the growth of zirconia grains adjacent to the spinel phase at temperatures higher than 1450°C, with transformation of zirconia from tetragonal phase into monoclinic phase. As a result of the large and faceted spinel grains existing in clusters and the large monoclinic zirconia grains, the phase transformation toughening effect of TZP diminished.

ACKNOWLEDGEMENT

This work was supported by the National Science Council, Taiwan, R.O.C., under contract number NSC-83-0405-E011-001.

REFERENCES

1. STEVENS, R., *Zirconia and Zirconia Ceramics*, 2nd edn. Magnesium Elektron Ltd., UK, 1986, pp.17–26.
2. LANGE, F. F., MARSHALL, D. B. & PORTER, J. R., Controlling microstructures through phase partitioning from metastable precursors: the $\text{ZrO}_2\text{--Y}_2\text{O}_3$ system. In *Ultrastructure Processing of Advanced Ceramics*, ed. J. D. Mackenzie & D. R. Ulrich. Wiley, NY, 1988, pp. 519–32.
3. WINNUST, A. J. A., THEYNISSEN, G. S. A. M., GROOT ZEVERT, W. F. M. & BURGGRAAF, A. J., The sintering behaviour of fine-grained $\text{ZrO}_2\text{--Y}_2\text{O}_3$ ceramics. In *Science of Ceramics, Vol. 14*, ed. D. Taylor. Institute of Ceramics, Stoke-on-Trent, UK, 1988, pp. 309–14.
4. CHEN, I. W. & XUE, L. A., Development of superplastic structural ceramics. *J. Am. Ceram. Soc.*, **73** (1990) 2585–609.
5. STOTO, T., NAUER, M. & CARRY, C., Influence of residual impurities on phase partitioning and grain growth processes of Y-TZP materials. *J. Am. Ceram. Soc.*, **74** (1991) 2615–21.
6. NAUER, M. & CARRY, C., Flow behaviours at high temperature of yttria doped zirconia polycrystals. In *Euro-Ceramics, Vol. 3*, ed. G. de With, R. A. Terpstra & R. Metselaar. Elsevier Applied Science, London, 1989, pp. 323–8.
7. FRENCH, J. D., CHAN, H. M., HARMER, M. P. & MILLER, G. A., Mechanical properties of interpenetrating microstructures: the $\text{Al}_2\text{O}_3\text{/c-ZrO}_2$ system. *J. Am. Ceram. Soc.*, **75** (1992) 418–23.
8. DILL, S., FRENCH, J. D., HARMER, M. P. & CHAN, H. M., Coarsening in duplex microstructures: the effect of liquid phase. *Bull. Am. Ceram. Soc.*, **71** (1992) 1554.
9. KISS, S. J. & KOSTIC, E., Phenomenological analysis of sintering in the presence of heterogeneities. *Powder Metall. Int.*, **24** (1992) 247–50.
10. KOSTIC, E., KISS, S. J. & BOSKOVIC, S., Sintering and microstructure development in the $\text{Al}_2\text{O}_3\text{--MnO--TiO}_2$ system. *Powder Metall. Int.*, **22** (1990) 29–30.
11. LIN, S. T., Sintering and injection molding of colored zirconia. National Science Council, Taiwan, R.O.C., NSC83-0405-E011-001, 1994.
12. HWANG, C. M. J. & CHEN, I. W., Effect of a liquid phase on the superplasticity of 2 mol% Y_2O_3 -stabilized tetragonal zirconia polycrystals. *J. Am. Ceram. Soc.*, **73** (1990) 1626–32.
13. HOWARD, C. J. & KISI, E. H., Polymorph method determination of monoclinic zirconia in partially stabilized zirconia ceramics. *J. Am. Ceram. Soc.*, **73** (1990) 3096–9.
14. EVANS, A. G. & CHARLES, E. A., Fracture toughness determinations by indentation. *J. Am. Ceram. Soc.*, **59** (1976) 371–2.
15. NORTON, F. H., *Elements of Ceramics*, 2nd edn. Addison-Wesley Pub. Co., Reading, MA, 1974, pp.126–7.
16. AUKRUST, E. & MUAN, A., The stability of $\text{CoO--Al}_2\text{O}_3$, $\text{CoO--Cr}_2\text{O}_3$, and 2CoO--SiO_2 . *J. Am. Ceram. Soc.*, **46** (1963) 358.
17. MASON, R. K., Use of cobalt colors in glazes. *Bull. Am. Ceram. Soc.*, **40** (1961) 5–6.
18. HANDWERKER, C. A., MORRIS, P. A. & COBLE, R. L., Effects of chemical inhomogeneity on grain growth and microstructure in Al_2O_3 . *J. Am. Ceram. Soc.*, **72** (1989) 130–6.
19. BAE, S. I. & BAIK, S., Determination of critical concentrations of silica and/or calcia for abnormal grain growth in alumina. *J. Am. Ceram. Soc.*, **76** (1993) 1065–7.
20. KURAMOTO, N., TANIGUCHI, H. & ASO, I., Development of translucent aluminum nitride ceramics. *Bull. Am. Ceram. Soc.*, **68** (1989) 883–7.
21. OH, Y. J., OH, T. S. & YUNG, H. J., Microstructure and mechanical properties of cordierite ceramics toughened by monoclinic ZrO_2 . *J. Mater. Sci.*, **28** (1991) 6491–5.
22. BUCHANAN, R. C. & WILSON, D. M., Role of Al_2O_3 in sintering of submicrometer yttria-stabilized ZrO_2 powders. In *Advances in Ceramics, Vol. 10, Structural and Properties of MgO and Al₂O₃ Ceramics*, ed. W. D. Kingery. American Ceramic Society, Columbus, OH, 1984, pp. 520–40.
23. LEVIN, E. M., *Phase Diagrams for Ceramists, Vol. III*, Figure 4378 and Figure 4568. American Ceramic Society, OH, 1975.
24. ZHOU, Y., LEI, T. C. & LU, Y. X., Grain growth and phase separation of $\text{ZrO}_2\text{--Y}_2\text{O}_3$ ceramics annealed at high temperature. *Ceram. Int.*, **18** (1992) 237–42.
25. GERMAN, R. M., *Liquid Phase Sintering*. Plenum Press, New York, 1985, pp. 13–39.
26. MECARTNEY, M. L., Influence of an amorphous second phase on the properties of yttria-stabilized tetragonal zirconia polycrystals (Y-TZP). *J. Am. Ceram. Soc.*, **70** (1987) 54–8.
27. HAASE, I., YI, L., NICHT, E. M., XIAOXIAN, H. & JINKUN, G., Preparation and characterization of ultra-fine zirconia powder. *Ceram. Int.*, **18** (1992) 343–51.